Published in final edited form as:
Anal Chem. 2005 July 15; 77(14): 4439–4447.

MALDI-TOF MS of Phosphorylated Lipids in Biological Fluids Using Immobilized Metal Affinity Chromatography and a Solid Ionic Crystal Matrix

Bryan M. Ham[†], **Jean T. Jacob**[‡], and **Richard B. Cole**[*,†]

†*Department of Chemistry, University of New Orleans, 2000 Lakeshore Drive, New Orleans, Louisiana 70148*

‡*Louisiana State University Health Sciences Center, Department of Ophthalmology, 2020 Gravier Street, Suite B, New Orleans, Louisiana 70112*

Abstract

When targeting a certain class of analytes, such as the phosphorylated lipids in complex biological extracts, interfering species can pose challenges to qualitative and quantitative analyses. Two aspects of lipid analysis were optimized to simplify the isolation and characterization of phosphorylated lipids in biological extracts. A new solid ionic crystal MALDI matrix was synthesized which combined the lipid response enhancing UV-absorber *p*-nitroaniline with the protonating agent butyric acid. Mass spectra of the extracts containing phosphorylated lipids were simplified by revealing only protonated molecules $[M + H]^+$ of the zwitterionic phosphatidylcholine (PC) headgroup-containing lipids, such as lyso-PC, PC, and platelet-activating factor. For the anionic phosphorylated lipids, such as phosphatidylglycerol, phosphatidic acid, and phosphatidylserine, further spectrum simplification is obtained by the appearance of only the monosodium adducts $[M + Na]^+$ as the major molecular ions, in preference to the double sodium adducts $[M + 2Na - H]^+$. In addition, a new extraction, isolation, and cleanup procedure has been developed to prepare the phosphorylated lipids for MALDI-TOF analysis by the use of immobilized metal ion affinity chromatography media (i.e., ZipTip). The latter procedure was successfully applied to a complex biological tear film lipid layer extract in preparation for MALDI-TOF analysis and phospholipid characterization.

Lipids are important biomolecules that are found in all living species. These include nonpolar lipids, such as the acylglycerols, and the more polar phosphorylated lipids. Of the nonpolar lipids, triacylglycerols are thought to be a storage form of energy in the cells,[1] whereas diacylglycerols are of special importance for their role as physiological activators of protein kinase C (PKC).[2,3] Of the polar lipids, those containing phosphoryl headgroups, such as the phosphatidylcholines (PC), the phosphatidylethanol-amines (PE), and the phosphatidylserines (PS) (see Figure 1 for structures), constitute the bilayer components of biological membranes, determine the physical properties of these membranes, and directly participate in membrane protein regulation and function. Other types of phosphorylated lipids are the sphingomyelins and the glycosphingolipids, which have been reported to be involved in different biological processes such as growth and morphogenesis of cells.[4] Thus, analysis of this special class of biomolecules has been of great interest to medical researchers, biologists, and chemists.

Recent analyses of phospholipids have employed HPLC;[5] MEKC;[5,6] CE-ES-MS;[7] ES-MS/MS;[8-15] and to a lesser extent, MALDI-FTICR[16] and MALDI-TOF.[17-21] The mass spectrometric analyses of nonvolatile lipids has been reviewed by Murphy et al.,[22] and it is pointed out that the advent of soft ionization techniques, such as ES-MS and MALDI-MS, has

*Corresponding author. Phone: (504) 280-7412. Fax: (504) 280-6860. E-mail: rcole@uno.edu.

obviated the need for derivatization of lipids. Biological samples are complex mixtures of a wide variety of compounds that can have a negative influence on the ability to identify and quantify lipids by mass spectrometry; effects include signal suppression and interferences from isomeric and isobaric compounds.

In this paper, a MALDI-TOF MS study of the phosphorylated lipids of normal human eye tear is reported using a novel solid ionic crystal MALDI matrix consisting of *p*-nitroaniline (PNA) and butyric acid. MALDI-TOF has become an important tool for the characterization of complex biological extracts due to its high sensitivity, high resolution, and limited fragmentation of the compounds of interest. Front-end isolation of the phosphorylated lipids was achieved using immobilized metal affinity chromatography (IMAC). The chemical composition of the human meibomian gland liquid secretions (tear) has previously been characterized by HPLC,[23] P NMR,[24] and TLC,[25] and fatty acid fragment profiles have been generated by HPLC/MS.[26] The newly developed methods reported in this paper enable the detection of very low levels of phosphorylated lipids in tear samples and have the potential for use for phosphorylated lipid determinations in other complex biological samples.

EXPERIMENTAL SECTION

Materials

Dimyristoyl phosphatidylcholine (DMPC), 1,2-dipalmitoyl-*sn*-glycero-3-phosphoethanolamine (DPPE), 1-palmitoyl-2-hydroxy-*sn*-glycero-3-phosphocholine (16:0-Lyso PC), (2*S*,3*R*,4*E*)-2-acylaminooctadec-4-ene-3-hydroxy-1-phosphocholine (brain, porcine, sphingomyelin, SM), L-α-phosphatidylinositol (PI, soy-sodium salt), 1-alkyl-2-acetoyl-*sn*-glycero-3-phosphocholine (platelet-activating factor, 16:0-PAF), 1-palmitoyl-2-oleoyl-*sn*-glycero-3-phosphate (PA, sodium salt), 1-palmitoyl-2-oleoyl-*sn*-glycero-3-[phospho-*rac*-(1-glycerol)] (PG, sodium salt), and 1-palmitoyl-2-oleoyl-*sn*-glycero-3-[phospho-L-serine] (PS, sodium salt) were purchased from Avanti Polar Lipids (Alabaster, AL). Monopentadecanoin, 1,3-dipentade-canoin, triheptadecanoin, and palmityl behenate were obtained from Nu-Chek Prep, Inc. (Elysian, MN) and had stated purities of >99%. 1-Stearoyl-2-palmitoylglycerol and 1-palmitoyl-2-stearoylglycerol, with stated purities of 99%, were purchased from Larodan Fine Chemicals AB (Malmo, Sweden). Cholesteryl stearate, 1,3-distearin, and 1-palmitoyl-3-stearoyl-*rac*-glycerol were purchased from Sigma Chemical Co. (St. Louis, MO). Methanol, acetonitrile, and chloroform solvents were of HPLC/spectroscopy grade and were purchased from EM Science (Darmstadt, Germany). All other chemicals were of analytical reagent grade, and all standards and chemicals were used as received without further purification. Distilled and deionized water (18 MΩ Milli-Q water system, Millipore Inc., Bedford, MA) was used throughout standard and sample preparations.

Extraction of Nonpolar and Polar Lipids

The nonpolar and polar lipid fractions were extracted from tear samples using a simple modified chloroform/water partitioning procedure.[27,28] The aqueous phase contained the tear proteins; the chloroform phase held the lipids.

Synthesis of Solid Ionic Crystal MALDI Matrix

Scheme 1 is a reaction scheme showing the synthesis of the solid ionic crystal matrix for MALDI. A 250-mg portion of 4-nitroaniline and 333 μL of butyric acid were added to 9.05 mL of methanol with vortex mixing. After 1 min, solvent was removed by rotary evaporation. Upon removal of the methanol, yellow, slightly oily, pungent crystals were formed. The MALDI matrix used for further studies consisted of 20 mg of the solid ionic crystal 4-nitroaniline/butyric acid dissolved in 1 mL of ethanol.

MALDI-TOF MS Analysis

MALDI-TOF mass spectra were acquired using an Applied Biosystems Voyager Elite r-ToF with delayed extraction (Applied Biosystems, Inc., Framingham, MA). An extraction voltage of 20 kV was typically employed. Delayed extraction mode was used for all acquisitions with a 175-ns delay time setting. The laser was operated just above the threshold energy required to obtain desorption/ionization. Each phospholipid mass spectrum constitutes an average of 150-200 traces. For sample plate spotting, 3 μL of phospholipid solution was mixed with 3 μL of matrix and then deposited onto the MALDI plate and allowed to air-dry.

All spectra were calibrated using a two-point calibration employing protonated 16:0-lyso PC, at *m*/*z* 496.34, and protonated 16:0/16:0-DMPC at *m*/*z* 678.51. Reported *m*/*z* values show nominal masses (i.e., values after the decimal place have been truncated). Phospholipids in the biological samples are assigned according to MALDI-TOF MS data, including molecular weights derived from either protonated molecules, or sodiated molecules, and PSD product ion data.

RESULTS AND DISCUSSION

Characterization and Optimization of the Solid Ionic Crystal MALDI Matrix

Experiments were performed to characterize and optimize the MALDI matrix for the mass spectral analysis of phosphorylated lipids extracted from tear samples. In general, prompt fragmentation involving cleavage at the headgroup of phosphorylated lipids is a common problem when analyzing biological lipid extracts by MALDI. Difficulties pertaining to the ability to obtain quantitative information also arise when using solid MALDI matrixes.[29] Inhomogeneous deposits of the analyte within the matrix and nonuniformities in the matrix layer cause variations in responses due to so-called “hot” or “sweet” spots versus the areas that produce lower-level signals. In general, a rather complex relationship exists between the MALDI spectral signal intensity and the amount of the measured analyte present in the spot.[30] A recent study by Rujoi et al.[20] reported the use of *p*-nitroaniline as a matrix for the study of neutral phospholipids (phosphatidylcholine and sphingomyelin) in lens tissue, where the obtained $[M + H]^+$, $[M + Na]^+$, and $[M + K]^+$ signals appeared in greater sensitivities as compared to the 2,5-dihydroxybenzoic acid (DHB) matrix often used for phosphorylated lipids. Recently reported by Mank et al.[29] is the use of ionic liquid matrixes which have improved shot-to-shot reproducibility of signal intensities over traditional solid matrixes. This should enable more accurate quantitative analysis by MALDI.[31] Also reported is a reduction in fragmentation induced by the MALDI technique when using the ionic liquid matrixes. Three examples of ionic liquid matrixes used by Mank et al.[29] are 2,5-dihydroxy benzoic acid butylamine, α-cyano-4-hydroxycinnamic acid butylamine, and 3,5-dimethoxy-4-hydroxycinnamic acid triethylamine. The ionic liquid matrixes are formed through combining the appropriate viscous liquid amines with the crystal MALDI matrix after having dissolved both in methanol. The methanol and free amine are subsequently removed, thus producing the ionic pair, which is then mixed with a small amount of ethanol to reduce the viscosity of the liquid matrix.

In the present study, *p*-nitroaniline was reacted with butyric acid, as shown in Scheme 1. This mixture contrasts with those reported by Mank et al. in that an ionic liquid was not produced. Rather, upon analyte mixing and drying, a *solid* ionic crystal is formed that acts as a powerful gas-phase proton donor and enhances phosphorylated lipid response. Because the final matrix preparation is crystalline, it shows deposition (spotting) behavior similar to other widely used solid MALDI matrixes, such as sinapinic acid, DHB, or α-CHCA. Furthermore, difficult applications, such as depositing the matrix upon tissue or other surfaces for MALDI analyses revealing two-dimensional spatial distributions,[32] will be more likely to succeed when a solid

ionic crystal matrix is used in preference to an ionic liquid matrix. Finally, acidification of the analyte environment should not be severe with the solid ionic crystal matrix (where butyric acid is largely ion-paired with a *p*-nitroaniline), in contrast to the acidic MALDI matrixes DHB or α-CHCA. This property can facilitate the analysis of certain compounds, such as plasmalogens, that are prone to hydrolysis in an acidic environment.

Zwitterionic Phospholipid MALDI Matrix Comparison

For the optimization of the MALDI matrix for phosphorylated lipid analyses, six matrix preparations were evaluated in a comparison of the PNA/butyric acid matrix (with and without TFA) to four standard matrix preparations. The six matrixes consisted of (1) 20 mg/mL DHB dissolved in 1:1 MeOH/$CHCl_3$, (2) 10 mg/mL DHB + 10 mg/mL α-CHCA + 0.1% TFA dissolved in 2:1 $CHCl_3$/MeOH, (3) 20 mg/mL PNA dissolved in EtOH, (4) 20 mg/mL PNA + 0.1% TFA dissolved in EtOH, (5) 20 mg/mL PNA/butyric acid ionic crystals dissolved in EtOH, and (6) 20 mg/mL PNA/butyric acid ionic crystals + 0.1% TFA dissolved in EtOH. TFA was included in certain preparations either to aid in analyte protonation, or to enhance the dissolution of the lipids in the matrix.[17]

Table 1 shows the zwitterionic phosphorylated lipids' major molecular ions observed in the MALDI spectra obtained using the six different matrixes; Figure 1 illustrates the structures of the phosphorylated lipids employed in this study. The left side of Figure 1 lists the neutral, "polar" zwitterionic phosphorylated lipids. The right side of Figure 1 shows the anionic phosphorylated lipids as their neutral sodium salts. In Table 1, the most striking feature found was that both the PNA/butyric acid matrix and the PNA/butyric acid plus TFA matrix produce the protonated form of (16:0/16:0)-PE as the predominant molecular ion. This is illustrated in Figure 2, which compares the MALDI spectra of (16:0/16:0)-PE using the six separate matrixes obtained at a laser fluence just above the threshold energy for appearance. For the DHB matrix, Figure 2a, the major molecular ion peak is the sodium adduct $[PE + Na]^+$ at *m*/*z* 714, whereas the protonated molecule $[PE + H]^+$ at *m*/*z* 692 is of considerably lower abundance in the spectrum. Also observed in the spectrum are major ions produced through neutral headgroup losses at *m*/*z* 537 $[PE + H - C_3H_{10}NO_4P]^+$ and at *m*/*z* 551 $[PE + H - C_2H_8NO_4P]^+$. The peak at *m*/*z* 564 is probably the result of postsource (metastable) decay prior to the reflectron (the peak is wide, and the isotopes are not resolved). The 1:1 DHB/α-CHCA plus TFA matrix, Figure 2b, produces the sodium adduct as the major molecular ion, but there is significant headgroup loss leading to *m*/*z* 551. The protonated molecule, $[PE + H]^+$, is only a very minor peak at *m*/*z* 692. The PNA matrix, Figure 2c, did not produce any appreciable positive mode molecular ions at the expected *m*/*z* values of sodium or proton adducts. The PNA plus TFA matrix, Figure 2d, did produce the protonated molecule $[PE + H]^+$ at *m*/*z* 692, but also major peaks for neutral losses of headgroup components at *m*/*z* 551 and *m*/*z* 605. In general, the inclusion of TFA was observed to promote fragmentation in the form of the loss of neutral headgroup components. The newly synthesized solid ionic crystal PNA/butyric acid matrix (Figure 2e) and the PNA/butyric acid plus TFA matrix (Figure 2f) were observed to produce protonated molecules (*m*/*z* 692) as the major spectral peaks, with only very minor amounts of sodium (*m*/*z* 714) and potassium (*m*/*z* 730) adducts. However, the presence of TFA was again observed to induce significant fragmentation of the protonated molecule in the form of headgroup (neutral) loss at *m*/*z* 551 (Figure 2f).

The observance of the protonated molecule, MH^+, as the major species in the mass spectrum helps to simplify spectral interpretation and can help enhance the fragmentation efficiency in tandem mass spectrometry experiments.[33] As illustrated in Table 1, the phosphatidylcholine headgroup containing lipids, such as lyso-PC, PC, PAF, and sphingomyelin, all yield protonated molecules as the predominant molecular ion for the six matrixes studied. However,

the solid ionic crystal PNA/butyric acid matrix allows formation of the strongest [lipid + H]$^+$ peak and is the least conducive to headgroup loss.

Figure 3a is a MALDI-TOF spectrum of the *p*-nitroaniline/butyric acid matrix preparation illustrating the low molecular weight matrix background ions. The predominant spectral PNA-related ions include: *m*/*z* 108 [PNA + H - HNO]$^+$ and *m*/*z* 109 [PNA + H - NO]$^{\bullet+}$ (both requiring rearrangement), *m*/*z* 122 [PNA + H - NH_3]$^+$, *m*/*z* 139 [PNA + H]$^+$, and *m*/*z* 229 [2PNA + H - H_2NO_2]$^{\bullet+}$ (actually produced through a reaction between two PNA molecules). Figure 3b is the MALDI-TOF spectrum of a two-component standard using the PNA/butyric acid matrix which includes the low molecular weight range of the spectrum. The standard consists of lyso PC and DMPC. As can be seen in Figure 3b, there is no interference of the matrix peaks with the lipid analytes. An approximate limit of detection was determined to be 1×10^{-6} M DMPC (~300 pg on sample target) using the novel solid ionic crystal as the MALDI matrix.

Anionic Phospholipid MALDI Matrix Comparison

Table 2 shows the anionic phosphorylated lipids' major molecular ions observed in MALDI mass spectra obtained using the six different matrixes (see right side of Figure 1 for structures). Row 1 of Table 2 shows the major molecular ions produced during MALDI-TOF MS analyses employing the six matrixes to desorb the lipid standard phosphatidylglycerol (16:0/18:1-PG) which is anionic and often present as a sodium salt. The DHB/α-CHCA plus TFA matrix was found to produce the [PG + 2Na - H]$^+$ molecular ion as the predominant peak, whereas the other five were observed to produce the sodium adduct [PG + Na]$^+$ as the predominant molecular ion. For the PNA plus TFA matrix, the addition of TFA was found to promote prompt headgroup loss from both [PG + 2Na - H]$^+$ and [PG + Na]$^+$. Figure 4a is the MALDI-TOF spectrum of 16:0/18:1-PG using the PNA/butyric acid matrix showing the sodium adduct [PG + Na]$^+$ at *m*/*z* 771 and [PG + 2Na - H]$^+$ at *m*/*z* 793. The phosphatidylserine lipid (16:0/18:1-PS) was also observed to suffer high degrees of headgroup loss with the addition of TFA, as shown in Table 2, row 2. For the DHB/α-CHCA plus TFA matrix, PS exhibited facile prompt headgroup loss, and [PS + Na]$^+$ at *m*/*z* 784 was observed to be a very minor spectral ion. Headgroup loss for PS leading to *m*/*z* 577 [PS - $C_3H_7NO_6PNa$]$^+$ as a major spectral ion was observed for the PNA plus TFA matrix and for the PNA/butyric acid plus TFA matrix. Figure 4b is the MALDI-TOF spectrum of PS using the PNA/butyric acid matrix showing [PS + Na]$^+$ at *m*/*z* 784 and [PS + 2Na - H]$^+$ at *m*/*z* 806. Notably, the phosphatidic acid (16:0/18:1-PA) lipid standard, Table 2, row 3, did not respond well when mixed with either the PNA matrix or the PNA/butyric acid plus TFA matrix. For PA in the PNA/butyric acid matrix (Figure 4c), the predominant ion peak was observed to be the [PA + Na]$^+$ ion at *m*/*z* 697, which is in contrast to the DHB/α-CHCA plus TFA matrix and the PNA plus TFA matrix, for which the predominant ion is [PA + 2Na - H]$^+$ (*m*/*z* 719). With the novel solid ionic crystal matrix (PNA/butyric acid), PG and PA are found predominantly as the sodium adducts [phospholipid + Na]$^+$, and not as [phospholipid + 2Na - H]$^+$. This suggests that the butyric acid additive in the PNA matrix is acting as a protonating agent during MALDI analysis, displacing one of the sodium ions. This behavior is similar to that observed for 16:0/16:0-PE (Table 1, row 1), in which the predominant molecular ion is [PE + H]$^+$ (Figure 2e), whereas the sodium adduct [PE + Na]$^+$ is observed as the predominant molecular ion with the DHB matrix (Figure 2a) and the DHB/α-CHCA plus TFA matrix (Figure 2b).

Other nonpolar lipids that do not contain phosphate in the headgroup were also tested with the new matrix. These consisted of cholesteryl stearate, monopentadecanoin, 1-palmitoyl-2-stearoylglycerol, 1-palmitoyl-3-stearoylglycerol, triheptadecanoin, and the wax ester palmityl behenate. Observed in the MALDI-TOF spectra (not shown) for all of these nonpolar lipids were sodium adducts as the predominant molecular ion peak, with minor potassium adducts.

As compared to traditional MALDI matrixes such as DHB for the study of phosphorylated lipids, one may summarize that the PNA/butyric acid solid ionic crystal offers (1) reliable appearance of only the protonated molecules of lipids containing phosphatidylcholine headgroups, such as lyso PC, PC, and PAF; (2) reliable appearance of only the sodium adduct species for anionic phospholipids, such as PG, PA, and PS; and (3) the ability to simultaneously detect all of the phosphorylated lipids represented in Figure 1 (including PE) in the positive mode of MALDI-MS. These three features can greatly simplify determinations of phosphorylated lipids present in complex biological samples and extracts.

PSD Fragmentation Study of Phosphatidylserine

Post-source decay (PSD) analysis was performed on the phosphorylated lipid standards to study the decompositions of $[\text{phospholipid} + H]^+$ for the neutral, polar zwitterionic phospholipids, and both the $[\text{phospholipid} + Na]^+$ and $[\text{phospholipid} + 2Na - H]^+$ peaks for the anionic phospholipids. Figure 5a is the PSD spectrum of the sodium adduct of phosphatidylserine (16:0/18:1-PS) $[PS + Na]^+$ at *m*/*z* 784. Figure 5b is the PSD spectrum of $[PS + 2Na - H]^+$ at *m*/*z* 806. As can be seen in the two figures, the two molecular ions of PS have the same fragmentation pathways producing loss of headgroup fragments, but the favored pathways appear to be quite different. The phosphatidylserine lipid under-goes three forms of headgroup neutral loss under PSD conditions. The three product ion structures representing *m*/*z* 697, 599, and 577 are illustrated in Figure 5a. According to a previous report by Al-Saad et al.,[19] *m*/*z* 577 may represent a six-membered ring product ion in which the sodium was lost with the headgroup. The *m*/*z* 599 product ion is assigned as the sodium adduct of a newly formed alkene. The fragmentation pathway leading to the *m*/*z* 577 product ion is clearly favored over the *m*/*z* 599 product ion (Figure 5a). The *m*/*z* 577 product ion involves the neutral loss of the sodium atom in the headgroup, whereas the production of the *m*/*z* 599 product ion results in the sodium remaining adducted to the acylglycerol portion of the lipid. This indicates that for each molecular ion that contains two sodium atoms, one of the sodium ions is clearly associated with the negatively charged oxygen in the phosphoryl group. Second, the pathway leading to the predominant *m*/*z* 208 product ion in Figure 5a, which consists of the neutral headgroup sodium adduct, is similar to the fragmentation pathway forming *m*/*z* 577, except that for *m*/*z* 208, a proton is transferred to the headgroup, so charge is retained on the latter. This further indicates that the predominant form of the precursor is the singly sodiated molecule where the sodium is adducted to the phosphoryl headgroup, not the acylglycerol portion of the lipid. For $[PS + 2Na - H]^+$ the only predominant product ion is *m*/*z* 719 (Figure 5b), which is formed through the neutral loss of $C_3H_5O_2N$ (87 Da). This indicates, as observed by Al-Saad et al.,[19] that $[PS + 2Na - H]^+$ is more stable than $[PS + Na]^+$. In fact, this is well-known because charge on Na^+ is less mobile than on H^+.[33] Figure 5b also contains structures of the different neutral molecules involved in headgroup losses.

PSD Fragmentation Study of Phosphatidic Acid

Headgroup-loss pathways similar to those observed for phosphatidylserine were also observed in the PSD spectrum of phosphatidic acid (16:0/18:1-PA), as illustrated in Figure 6a. In the spectrum, there is the six-membered ring formation for the neutral loss of the sodium-containing headgroup at *m*/*z* 577 $[M + Na - PO_4H_2Na]^+$, and the alkene product ion formed through neutral headgroup loss at *m*/*z* 599 $[M + Na - PO_4H_3]^+$. Also observed in Figure 6a are product ion peaks arising from neutral loss of the C16:0 fatty acid substituent at *m*/*z* 441 $[M + Na - C_{16}H_{32}O_2]^+$, neutral loss of C18:0 sodium fatty acetate at *m*/*z* 391 $[M + Na - C_{18}H_{35}O_2Na]^+$, and a sodium adduct of the phosphoric acid headgroup at *m*/*z* 121 $[H_3PO_4Na]^+$. Figure 6b is the PSD spectrum of $[PA + 2Na - H]^+$. The two predominant peaks are formed through neutral losses of the fatty acid substituents and can be used for identification purposes when coupled with the PSD spectrum of $[PA + Na]^+$, which gives headgroup information.

PSD Fragmentation Study of Lyso PC and DMPC

Figure 7a is the PSD spectrum of protonated lyso 1-palmitoyl choline (16:0-lyso PC) at *m*/*z* 496. The predominant product ion in the spectrum is the expected peak representing the protonated phosphatidylcholine headgroup at *m*/*z* 184; however, there are three other peaks of interest in the spectrum. The *m*/*z* 313 peak is derived from the neutral loss of the phosphatidylcholine headgroup from the *m*/*z* 496 precursor $[M + H - C_5H_{14}NO_4P]^+$ and the *m*/*z* 258 peak from the neutral loss of a fatty acyl chain as a ketene $[M + H - C_{16}H_{30}O]^+$. The observance of these two peaks can aid in the identification of the lyso phosphatidylcholine lipid. The third peak at *m*/*z* 104 is the headgroup fragment ion $C_5H_{14}NO^+$, whose structure is illustrated in Figure 7a. Figure 7b is the PSD spectrum of protonated dimyristoyl phosphatidylcholine (14:0/14:0-DMPC) at *m*/*z* 678. In this spectrum, there is also the *m*/*z* 184 product ion for the charged phosphatidylcholine headgroup that has previously been reported by Al-Saad et al.[34] and a *m*/*z* 495 product ion derived from neutral loss of the PC headgroup $[M + H - C_{14}H_{14}NO_4P]^+$. For fatty acid substituent identification, there is the product ion at *m*/*z* 450 derived from the neutral loss of the C14:0 fatty acid $[M + H - C_{14}H_{28}O_2]^+$ and a product ion at *m*/*z* 468 from the neutral loss of a C14:0 fatty acyl chain as a ketene $[M + H - C_{14}H_{26}O]^+$. At *m*/*z* 86 in the spectrum there is a PC headgroup product ion whose structure is illustrated in Figure 7b.

PSD Fragmentation Study of Phosphatidylglycerol

Figure 8a is the PSD spectrum of the sodium adduct of 1-palmitoyl-2-oleoyl-*sn*-glycero-3-[phospho-*rac*-(1-glycerol)] (sodium salt) (16:0/18:1-POPG) at *m*/*z* 771. In the spectrum, there are three predominant product ion peaks which involve the phosphoglycerol headgroup. At *m*/*z* 599, there is a minor peak for the neutral loss of the phosphoglycerol headgroup, and at *m*/*z* 577 there is the more predominant product ion peak for neutral loss of the phosphoglycerol headgroup (with sodium). The fact that the intensity of the *m*/*z* 577 peak is greater than that of the *m*/*z* 599 peak suggests that the departure of the neutral headgroup (with sodium) is the more favored fragmentation pathway, as was also observed in the PSD of 16:0/18:1-PS (Figure 5a). The most predominant product ion peak in the spectrum is the *m*/*z* 195 peak, that is, the sodium adduct of the phosphoglycerol headgroup whose structure is illustrated in Figure 8a. A minor peak is also observed at *m*/*z* 415, representing a two-step loss of a headgroup fragment (neutral loss of 74 Da; see Figure 8b, *m*/*z* 719 structure) in conjunction with neutral loss of the C18:1 fatty acid substituent $[M + Na - C_3H_6O_2 - C_{18}H_{34}O_2]^+$, giving some structural information for the phosphorylated lipid. Figure 8b is the PSD spectrum of 16:0/18:1-PG $[PG + 2Na - H]^+$ at *m*/*z* 793. This spectrum contains information concerning both the phosphoglycerol headgroup and the two fatty acid substituents. Those peaks at *m*/*z* 719, *m*/*z* 217, and *m*/*z* 199 involve cleavages of the phosphoglycerol headgroup and the associated structures are represented in the spectrum. The two fatty acid substituents are identified in the spectrum through two separate fragmentation pathways. There is a product ion formed as a result of neutral loss of the C18:1 fatty acid at *m*/*z* 511 $[M - H + 2Na - C_{18}H_{34}O_2]^+$ and a product ion formed upon neutral loss of the C16:0 fatty acid at *m*/*z* 537 $[M - H + 2Na - C_{16}H_{32}O_2]^+$. There are also two product ion peaks at *m*/*z* 437 and *m*/*z* 463 representing the combined neutral losses of a headgroup fragment and a fatty acid for the C18:1 and the C16:0 fatty acyl substituents, respectively.

IMAC Cleanup and Preconcentration of Phosphorylated Lipids

A modified Millipore phosphopeptide enrichment method using ZipTip (Millipore Inc., Bedford, MA) pipet tips containing an immobilized metal ion affinity chromatography (IMAC) media (iminodiacetic acid, IDA resin) was used to enrich the phosphorylated lipids. The suggested method from the manufacturer was followed except for two key solutions: the binding solution was changed from 0.1% acetic acid (aqueous) to 0.1% acetic acid in 1:1 methanol/acetonitrile, and the elution solution was changed from 0.3 N ammonium hydroxide

(aqueous) to 0.3 N ammonium hydroxide in 1:1 methanol/acetonitrile. The immobilized metal ion affinity chromatography (IMAC) media was found to be soluble in chloroform; therefore, care must be taken to remove all chloroform from the extracted lipids before application of the ZipTip.

Figure 9 is a MALDI-TOF MS spectrum illustrating the recovery of a four-component lipid standard mixture consisting of 16:0-lyso phosphatidylcholine at *m*/*z* 496, 14:0/14:0-dimyristoyl phosphatidylcholine at *m*/*z* 678, 16:0/16:0-dipalmitoyl phosphatidylethanolamine at *m*/*z* 692, and 16:0-sphingomyelin at *m*/*z* 731, each detected in protonated form using the modified IMAC ZipTip method. The peak at *m*/*z* 733 is likely to represent a reduced form of 16:0-sphingomyelin. The modified IMAC ZipTip method presented in this study has, thus, been demonstrated to be applicable to the isolation and cleanup of phosphorylated lipids in addition to the manufacturer's intended use for the isolation and cleanup of phosphorylated peptides.

MALDI-TOF MS Analysis of Human Tear Film Lipid Layer

A normal eye tear sample was extracted, using the modified extraction procedure above, forming a chloroform phase containing lipids and an aqueous phase containing proteins. The chloroform phase was evaporated, and the phosphorylated lipids were isolated using the IMAC ZipTip method. Figure 10a is a MALDI-TOF spectrum of the tear total chloroform extractables acquired without the use of the IMAC ZipTip cleanup method. Figure 10b is the same extract with the use of the IMAC ZipTip cleanup prior to spectral acquisition. In Figure 10a, the major peaks observed have been previously identified in our laboratory[35] as sodium adducts of monopalmitin at *m*/*z* 353 (not shown), monostearin at *m*/*z* 381 (not shown), a glyceryl/isoprene acetal at *m*/*z* 437, 1,3-dipalmitin at *m*/*z* 591, 1-stearoyl,3-palmitoylglycerol at *m*/*z* 619, and 1,3-distearin at *m*/*z* 647. As has been observed previously in our laboratory with electrospray, the phosphorylated lipids are present in tear extracts in very low concentrations compared to the acylglycerols, and they can experience a substantial amount of, or even complete, signal suppression in positive mode electrospray. Figure 10a illustrates that signal suppression of the phosphorylated lipids in the tear extract, due to the acylglycerols present, is also occurring with the use of MALDI. By applying the IMAC ZipTip isolation and cleanup procedure to the phosphorylated lipids, removal of the acylglycerols has been achieved, and the phosphorylated lipids are now observable in Figure 10b. In the ZipTip extract cleanup spectrum of Figure 10b, *m*/*z* 659 is postulated to be the sodium adduct of a pyrophosphate sphingomyelin with a molecular formula of $C_{24}H_{50}N_2O_{13}P_2Na$, *m*/*z* 678 is assigned as protonated 1,2-(*rac*)-dimyristoyl phosphatidylcholine, and *m*/*z* 719 and 747 are also postulated to be protonated pyrophosphate sphingomyelins with molecular formulas of $C_{31}H_{65}N_2O_{12}P_2$ and $C_{33}H_{69}N_2O_{12}P_2$, respectively. There are also even-numbered ions at *m*/*z* 430 and 530, indicating an odd number of nitrogens in those unidentified compounds.

CONCLUSIONS

Biological extracts, such as the tear film lipid layer presented in this study, are typically complex, multicomponent mixtures. Separation schemes are usually employed to isolate the compounds of interest, to simplify the mass spectra, and to lower the limits of detection. The novel solid ionic crystal MALDI matrix reported in this paper combines lipid detection enhancement through the use of *p*-nitroaniline as the matrix's ultraviolet light absorber with the powerful protonating additive butyric acid. Mass spectrum complexity is reduced, and interpretation is simplified due to the phosphorylated lipids of interest exhibiting primarily $[M + H]^+$ ions for the neutral, polar, zwitterionic phosphatidylcholine headgroup containing species lyso PC, PC, SM, and PAF. Further simplification is obtained because one need only monitor the mass spectrum for sodium adducts of the anionic phosphorylated lipids such as

PG, PA, and PS. Finally, all of the phosphorylated lipids represented in this study can be measured simultaneously in the positive mode, including PE. It has also been demonstrated that the new ionic crystal matrix allows the acquisition of PSD spectra that can be used for headgroup identification and fatty acid substituent characterization for both the nitrogen-containing phosphorylated lipids and those devoid of nitrogen.

A new extraction, isolation, and cleanup procedure has also been reported for the phosphorylated lipids using immobilized metal ion affinity chromatography (IMAC) media ZipTip. It was shown that the ZipTip procedure is highly specific for recovery of the phosphorylated lipids. The ZipTip procedure has been successfully applied to a complex biological tear film lipid layer extract by removing the signal suppressing acylglycerols, thus allowing the determination of very low levels of phosphorylated lipids.

ACKNOWLEDGMENT

Financial support was provided by The Louisiana Board of Regents through grant no. LEQSF (2001-04)-RD-B-11, the National Science Foundation CHE-0518288, the National Eye Institute through NEI/R03 EY0114021 and P30 E4002377, and from Research to Prevent Blindness.

References

(1). Ohlrogge J, Browse J. Plant Cell 1995;7:957–970. [PubMed: 7640528]

(2). Hodgkin MN, Pettitt TR, Martin A, Wakelam MJO. Biochem. Soc. Trans 1996;24:991–994. [PubMed: 8968498]

(3). Pettitt TR, Martin A, Horton T, Liassis C, Lord JM, Wakelam MJO. J. Biol. Chem 1997;272:17354–17359. [PubMed: 9211874]

(4). Gu M, Kerwin JL, Watts JD, Aebersold R. Anal. Biochem 1997;244:347–356. [PubMed: 9025952]

(5). Szucs R, Verleysen K, Duchateau GSMJE, Sandra P, Vandeginste BGM. J. Chromatogr., A 1996;738:25–29.

(6). Verleysen K, Sandra P. J. High Resolut. Chromatogr 1997;20:337–339.

(7). Raith K, Wolf R, Wagner J, Neubert RHH. J. Chromatogr., A 1998;802:185–188.

(8). Han X, Gross RW. J. Am. Chem. Soc 1996;118:451–457.

(9). Hoischen C, Ihn W, Gura K, Gumpert J. J. Bacteriol 1997;179:3437–3442. [PubMed: 9171385]

(10). Hsu FF, Bohrer A, Turk J. J. Am. Soc. Mass Spectrom 1998;9:516–526. [PubMed: 9879366]

(11). Khaselev N, Murphy RC. J. Am. Soc. Mass Spectrom 2000;11:283–291. [PubMed: 10757164]

(12). Hsu FF, Turk J. J. Mass Spectrom 2000;35:596–606.

(13). Liebisch G, Drobnik W, Lieser B, Schmitz G. Clin. Chem 2002;48:2217–2224. [PubMed: 12446479]

(14). Ho YP, Huang PC, Deng KH. Rapid Commun. Mass Spectrom 2003;17:114–121. [PubMed: 12512089]

(15). Hsu FF, Turk J. J. Am. Soc. Mass Spectrom 2004;15:1–11. [PubMed: 14698549]

(16). Marto JA, White FM, Seidomridge S, Marshall AG. Anal. Chem 1995;67:3979–3984. [PubMed: 8633761]

(17). Schiller J, Arnhold J, Benard S, Muller M, Reichl S, Arnold K. Anal. Biochem 1999;267:46–56. [PubMed: 9918654]

(18). Ishida Y, Nakanishi O, Hirao S, Tsuge S, Urabe J, Sekino T, Nakanishi M, Kimoto T, Ohtani H. Anal. Chem 2003;75:4514–4518. [PubMed: 14632058]

(19). Al-Saad KA, Zabrouskov V, Siems WF, Knowles NR, Hannan RM, Hill HH Jr. Rapid Commun. Mass Spectrom 2003;17:87–96. [PubMed: 12478559]

(20). Rujoi M, Estrada R, Yappert MC. Anal. Chem 2004;76:1657–1663. [PubMed: 15018564]

(21). Woods AS, Ugarov M, Egan T, Koomen J, Gillig KJ, Fuhrer K, Gonin M, Schultz JA. Anal. Chem 2004;76:2187–2195. [PubMed: 15080727]

(22). Murphy RC, Fiedler J, Hevko J. Chem. Rev 2001;101:479–526. [PubMed: 11712255]

(23). Ohyama T, Matsubara C, Takamura K. Analyst 1996;121:1943–1947. [PubMed: 9008409]
(24). Greiner JV, Glonek T, Korb DR, Booth R, Leahy CD. Ophthalmic Res 1996;28:44–49. [PubMed: 8726676]
(25). Wollensak G, Mur E, Mayr A, Baier G, Gottinger W, Stoffler G. Graefe's Arch. Clin. Exp. Ophthalmol 1990;228:78–82.
(26). Sullivan BD, Evans JE, Krenzer KL, Dana MR, Sullivan DA. JCEM 2000;85:4866–4875. [PubMed: 11134155]
(27). Folch J, Lees M, Stanley GHS. J. Biol. Chem 1957;226:497–509. [PubMed: 13428781]
(28). Bligh EG, Dyer WJ. Can. J. Biochem. Physiol 1959;37:911–917. [PubMed: 13671378]
(29). Mank M, Stahl B, Boehm G. Anal. Chem 2004;76:2938–2950. [PubMed: 15144208]
(30). Aebersold R, Mann M. Nature 2003;422:198–207. [PubMed: 12634793]
(31). Li YL, Gross ML. J. Am. Soc. Mass Spectrom 2004;12:1833–1837. [PubMed: 15589759]
(32). Luxembourg SL, McDonnell LA, Duursma MC, Guo X, Heeren RMA. Anal. Chem 2003;75:2333–2341. [PubMed: 12918974]
(33). Cole RB, Tabet J, Blais J. Int. J. Mass Spectrom. Ion Processes 1990;98:269–283.
(34). Al-Saad KA, Siems WF, Hill HH, Zabrouskov V, Knowles NR. J. Am. Soc. Mass Spectrom 2003;14:373–382. [PubMed: 12686484]
(35). Ham BM, Jacob JT, Keese MM, Cole RB. J. Mass Spectrom 2004;39:1321–1336. [PubMed: 15532045]

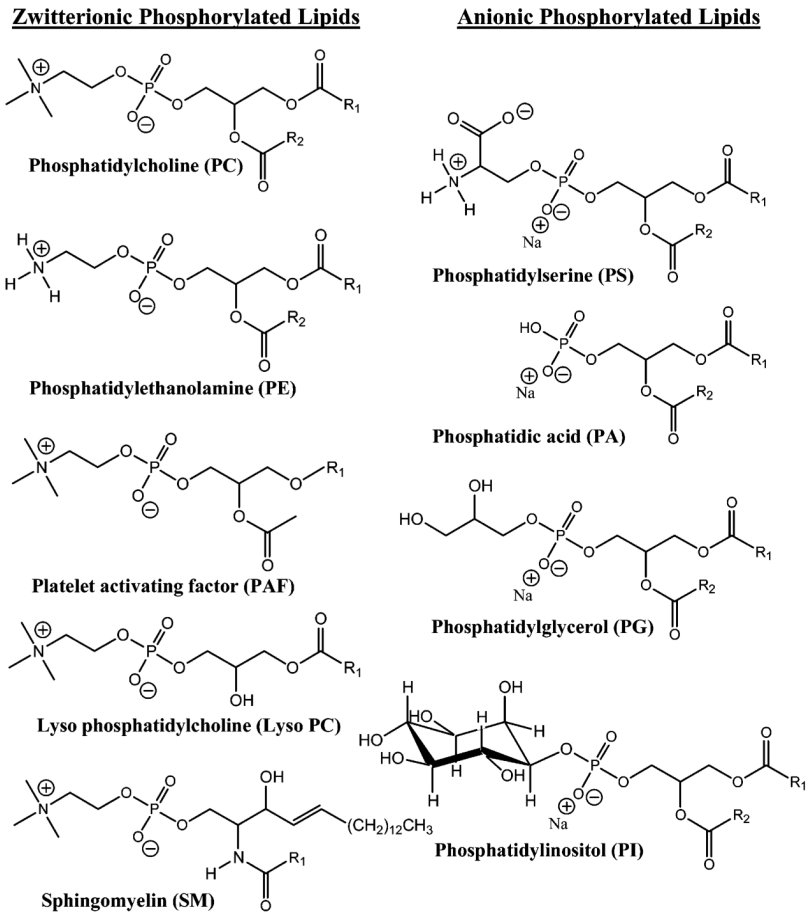

Figure 1.
Structures of the main phosphorylated lipids included in this study.

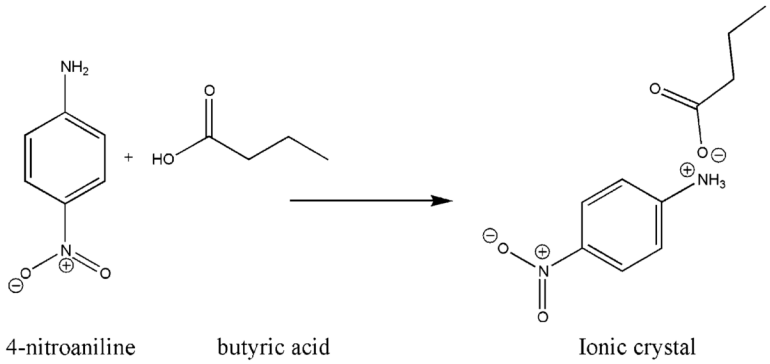

Scheme 1.
Synthesis of the Solid Ionic Crystal Matrix for MALDI.

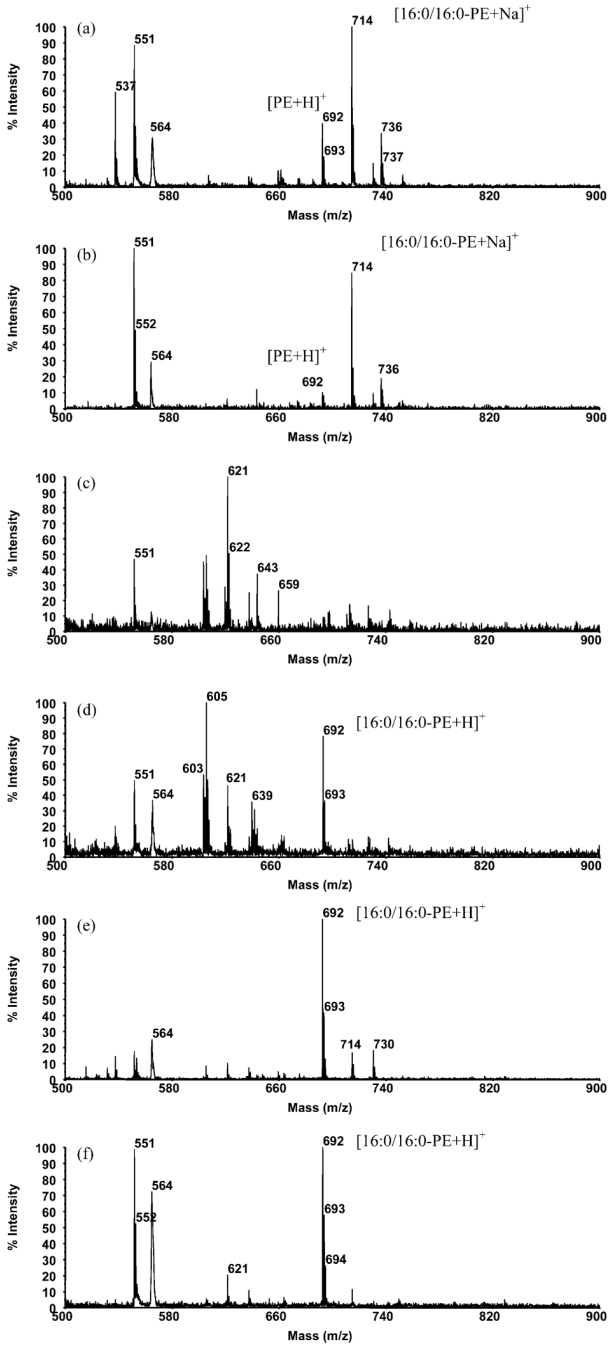

Figure 2.

Comparison of the six MALDI matrixes for the analysis of 16:0/16:0-phosphatidylethanolamine in positive ion mode. (a) DHB matrix showing predominant sodium adduct peak $[PE + Na]^+$ at *m/z* 714 and minor $[PE + H]^+$ at *m/z* 692. (b) α-CHCA/DHB plus TFA matrix with sodium adduct at *m/z* 714, but significant headgroup loss at *m/z* 551 observed, and a minor $[PE + H]^+$ peak at *m/z* 692. (c) PNA matrix shows no appreciable signals for sodium adducts or protonated molecules. (d) PNA plus TFA producing $[PE + H]^+$ at *m/z* 692, but major peaks for neutral losses of headgroup components at *m/z* 551, and *m/z* 605 are also observed. (e) PNA/butyric acid solid ionic crystal matrix producing predominantly the $[PE + H]^+$ ion at *m/z* 692 with only very minor amounts of the sodium and potassium adducts at *m/*

z 714 and *m*/*z* 730 and few fragment ions. (f) PNA/butyric acid plus TFA matrix producing the $[PE + H]^+$ ion at *m*/*z* 692 as a major spectral peak, but also significant headgroup loss ions at *m*/*z* 551 and *m*/*z* 564.

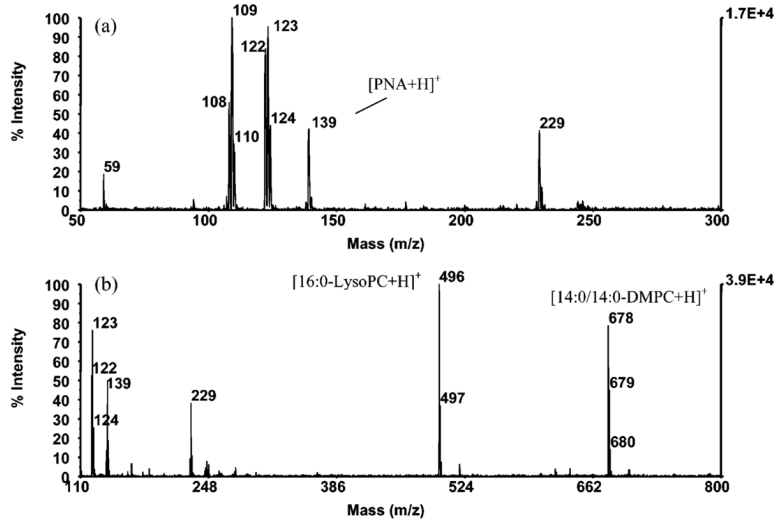

Figure 3.

(a) MALDI-TOF mass spectrum of the *p*-nitroaniline/butyric acid matrix preparation illustrating the low-mass region of the mass spectrum and showing background peaks originating from the matrix. (b) MALDI-TOF mass spectrum of a two-component mixture of 16:0-lyso PC and 14:0/14:0-DMPC standards showing protonated 16:0-lyso PC at *m*/*z* 496 and protonated 14:0/14:0-DMPC at *m*/*z* 678 using the PNA/butyric acid matrix.

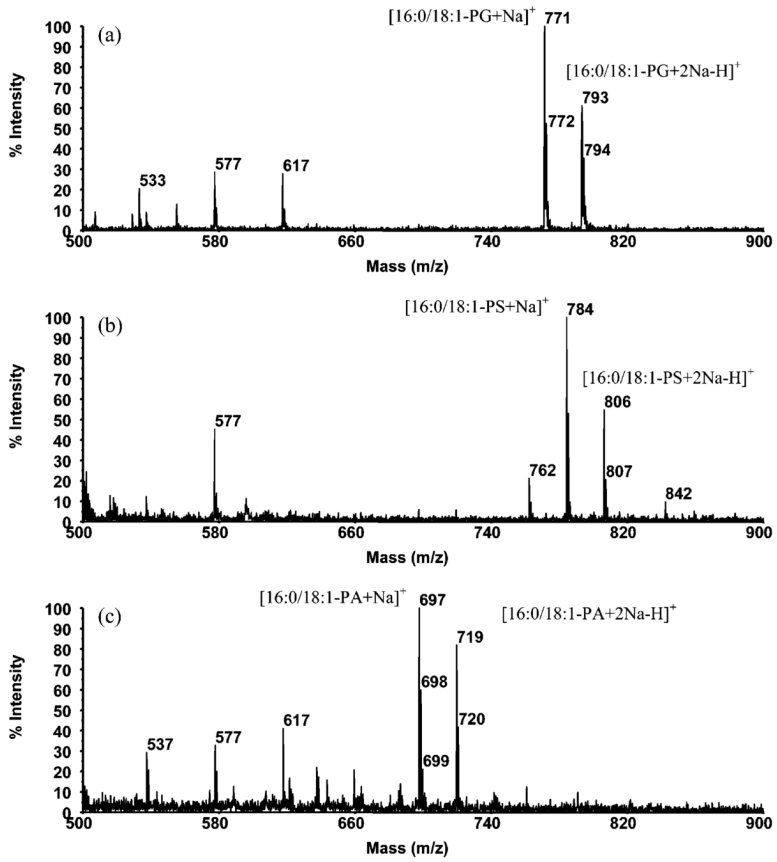

Figure 4.

(a) MALDI-TOF mass spectra acquired using the PNA/butyric acid matrix: (a) 16:0/18:1-PG showing $[PG + Na]^+$ at *m*/*z* 771 and $[PG + 2Na - H]^+$ at *m*/*z* 793, (b) 16:0/18:1-PS displaying $[PS + Na]^+$ at *m*/*z* 784 and $[PS + 2Na - H]^+$ at *m*/*z* 806, and (c) 16:0/18:1-PA showing $[PA + Na]^+$ at *m*/*z* 697 and $[PA + 2Na - H]^+$ at *m*/*z* 719.

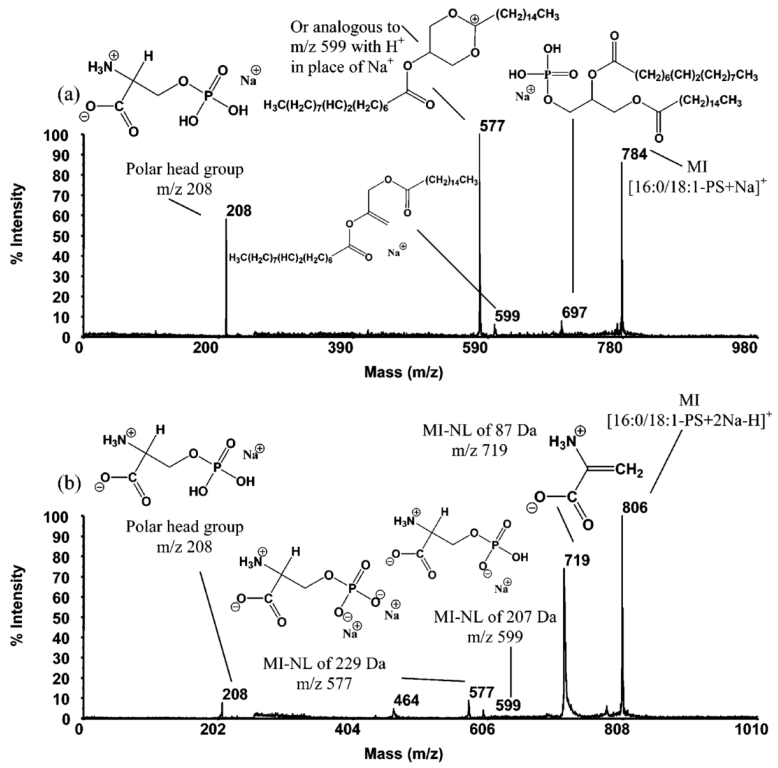

Figure 5.

PSD spectra of (a) 16:0/18:1-phosphatidylserine $[PS + NA]^+$ precursor ion at *m/z* 784 and (b) 16:0/18:1-phosphatidylserine $[PS + 2Na - H]^+$ precursor ion at *m/z* 806.

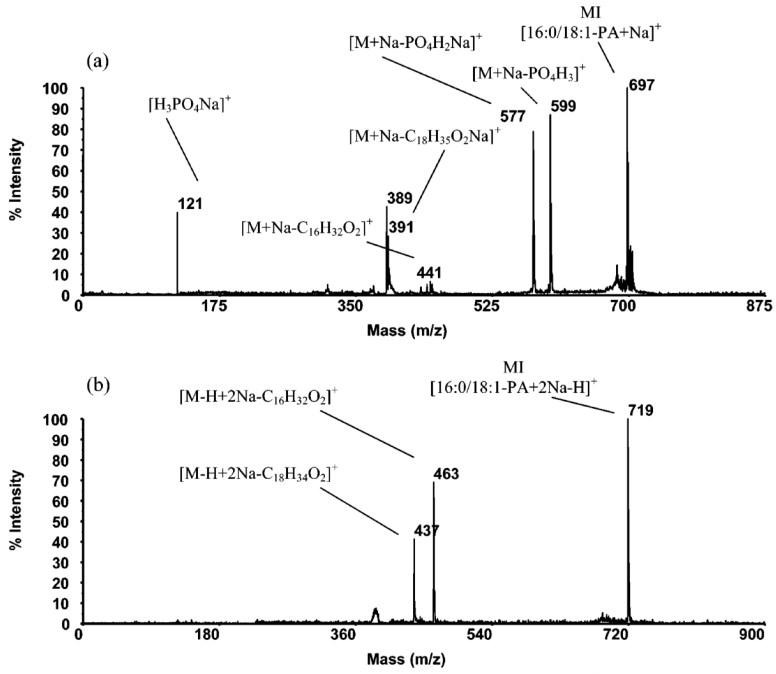

Figure 6.

PSD spectra of (a) 16:0/18:1-phosphatidic acid $[PA + NA]^+$ precursor ion at *m*/*z* 697 and (b) 16:0/18:1-phosphatidic acid $[PA + 2Na - H]^+$ precursor ion at *m*/*z* 719.

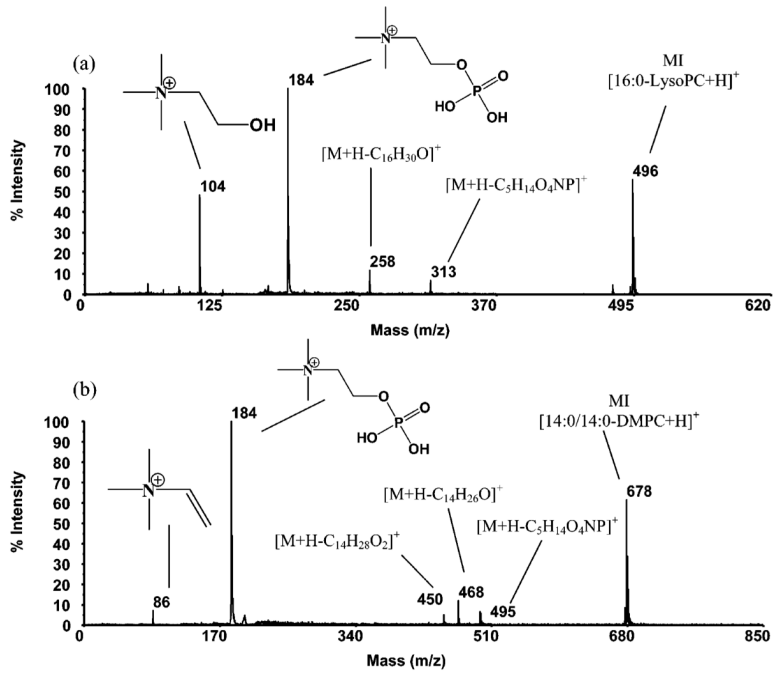

Figure 7.

PSD spectra of (a) lyso 1-palmitoyl choline (16:0-lyso PC) $[\text{Lyso PC} + \text{H}]^+$ precursor ion at *m*/*z* 496 and (b) dimyristoyl phosphatidylcholine (14:0/14:0-DMPC) $[\text{DMPC} + \text{H}]^+$ precursor ion at *m*/*z* 678.

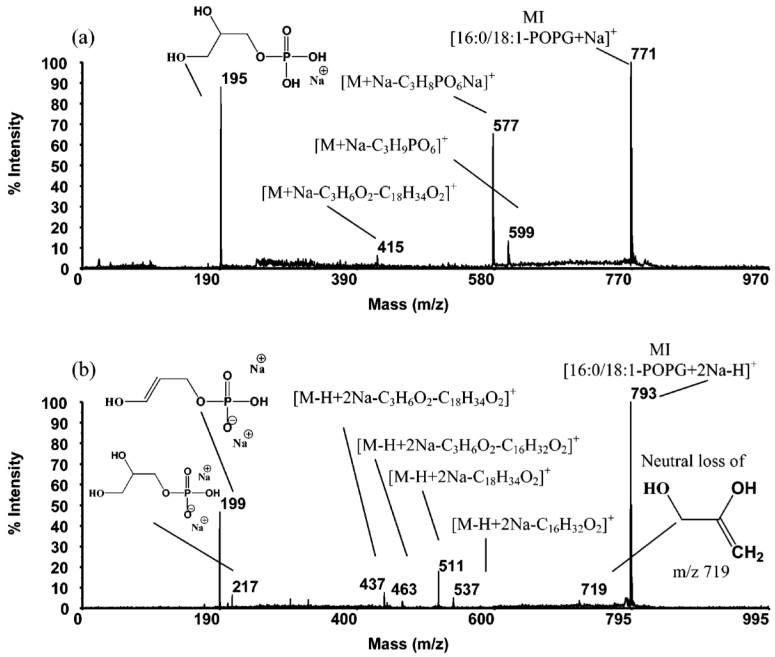

Figure 8.

PSD spectra of (a) 1-palmitoyl-2-oleoyl-*sn*-glycero-3-[phospho-*rac*-(1-glycerol)] (16:0/18:1-POPG) $[POPG + Na]^+$ precursor ion at *m*/*z* 771 and (b) $[POPG + 2Na - H]^+$ precursor ion at *m*/*z* 793.

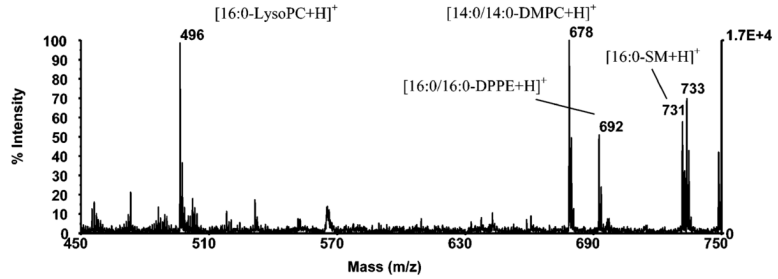

Figure 9.

Recovery of a four-component phosphorylated lipid standard mixture using the IMAC ZipTip. Protonated 16:0-lyso phosphatidylcholine at *m*/*z* 496, protonated dimyristoyl phosphatidylcholine at *m*/*z* 678, protonated dipalmitoyl phosphatidylethanolamine at *m*/*z* 692, and protonated 16:0-sphingomyelin at *m*/*z* 731.

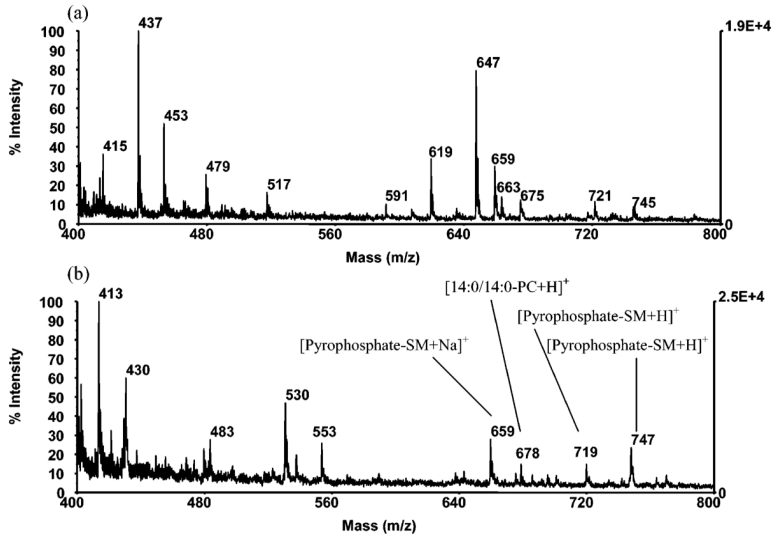

Figure 10.

MALDI-TOF mass spectra of the tear total chloroform extractables acquired (a) without the use of the IMAC ZipTip cleanup method and (b) with the use of the IMAC ZipTip cleanup prior to spectral acquisition.

Table 1

Comparative Study of the Zwitterionic Phosphorylated Lipids' Major Spectral Molecular Ions Observed for the Six Different MALDI Matrixes[a]

lipid	DHB	50/50 αCHCA/DHB, 0.1% TFA	PNA	PNA, 0.1% TFA	PNA + butyric acid	PNA + butyric acid, 0.1% TFA
16:0/16:0-PE	$[PE + Na]^+$ $[PE - HG]^+$	$[PE + Na]^+$ $[PE - HG]^+$	very low signal	$[PE + H]^+$ $[PE - HG]^+$	$[PE + H]^+$	$[PE + H]^+$ $[PE - HG]^+$
16:0-Lyso PC	$[PC + H]^+$ $[PC + Na]^+$	$[PC + H]^+$	$[PC + H]^+$	$[PC + H]^+$	$[PC + H]^+$	$[PC + H]^+$
16:0-SM	$[SM + H]^+$ $[SM + Na]^+$	$[SM + H]^+$	$[SM + H]^+$	$[SM + H]^+$	$[SM + H]^+$	$[SM + H]^+$
14:0/14:0-PC	$[PC + H]^+$	$[PC + H]^+$	$[PC + H]^+$	$[PC + H]^+$	$[PC + H]^+$	$[PC + H]^+$
16:0-PAF	$[PAF + H]^+$	$[PAF + H]^+$	$[PAF + H]^+$	$[PAF + H]^+$	$[PAF + H]^+$	$[PAF + H]^+$

[a] For abbreviations, see text. HG = headgroup.

Table 2

Comparative Study of the Anionic Phosphorylated Lipids' Major Spectral Molecular Ions Observed for the Six Different MALDI Matrixes[a]

lipid	DHB	50/50 αCHCA/ DHB, 0.1% TFA	PNA	PNA, 0.1% TFA	PNA + butyric acid	PNA + butyric acid, 0.1% TFA
16:0/18:1-PG	$[PG + Na]^+$ $[PG + 2Na - H]^+$ $[PG - HG]^+$	$[PG + 2Na - H]^+$	$[PG + Na]^+$ $[PG + 2Na - H]^+$	$[PG + Na]^+$ $[PG + 2Na - H]^+$ $[PG - HG]^+$	$[PG + Na]^+$ $[PG + 2Na - H]^+$	$[PG + Na]^+$
16:0/18:1-PS	$[PS + Na]^+$ $[PS + 2Na - H]^+$	$[PS - HG]^+$	$[PS + Na]^+$	$[PS + Na]^+$ $[PS - HG]^+$	$[PS + Na]^+$	$[PS - HG]^+$
16:0/18:1-PA	$[PA + Na]^+$ $[PA + 2Na - H]^+$	$[PA + 2Na - H]^+$	very low signal	$[PA + 2Na - H]^+$ $[PA + Na]^+$	$[PA + Na]^+$ $[PA + 2Na - H]^+$	very low signal
16:0/18:2-PI	$[PI + Na]^+$ $[PI + 2Na - H]^+$	$[PI + 2Na - H]^+$ $[PI + Na]^+$	$[PI + Na]^+$ $[PI + 2Na - H]^+$	$[PI + Na]^+$ $[PI + 2Na - H]^+$	$[PI + Na]^+$ $[PI + 2Na - H]^+$	$[PI + Na]^+$ $[PI + 2Na - H]^+$

[a] For abbreviations, see text. HG = headgroup.

Anal Chem. Author manuscript; available in PMC 2008 February 4.